Fluid Phenomena: Some Examples

1. Stellar Physics

Ordinary Star:

Self-gravitating, rotating, gaseous sphere

Radius changes on time scales of 10^{10} years

Collapse in 10^3 s in absence of gas pressure

Solar granulation: 5 minute time scale

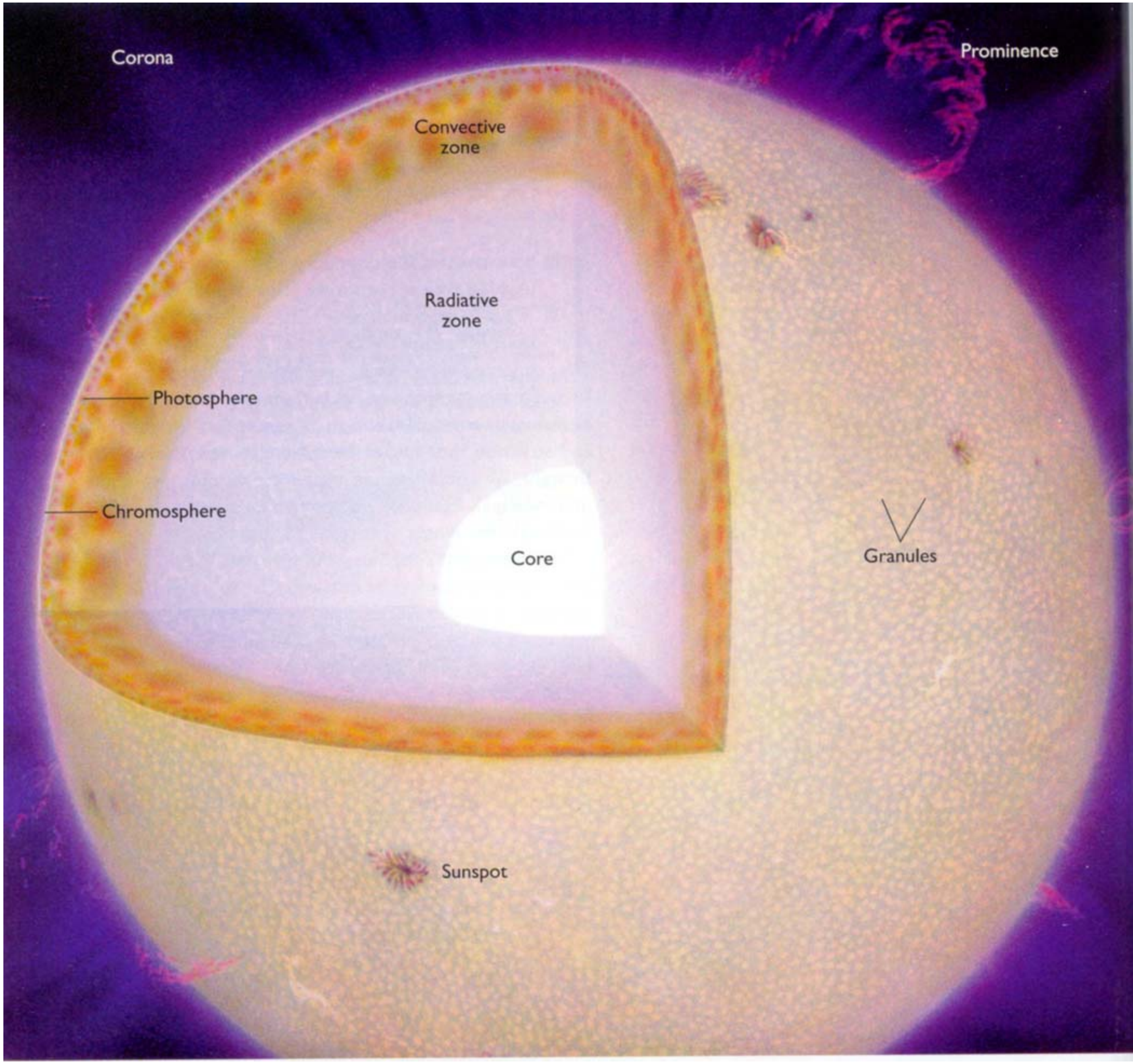

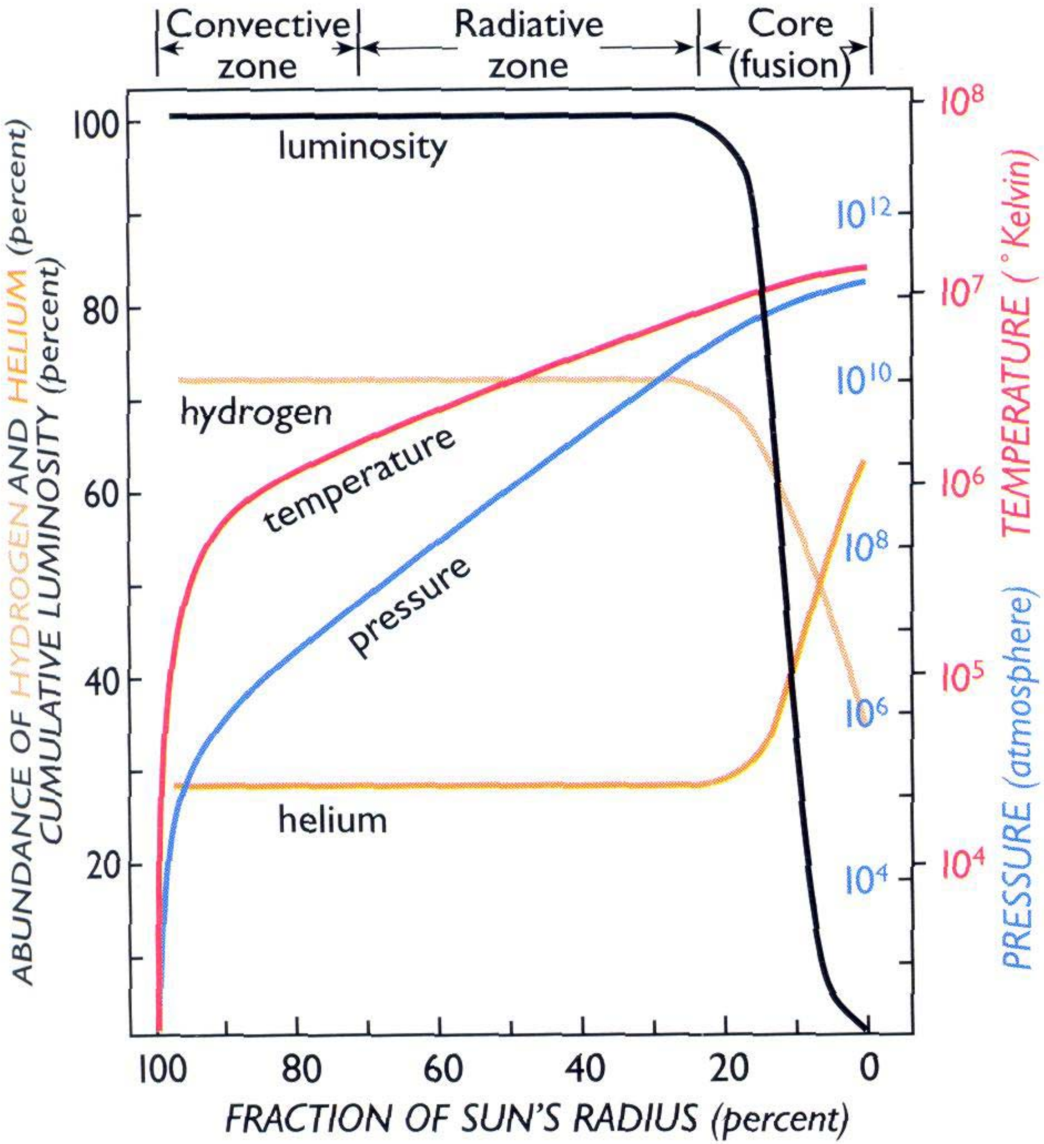

Figure 2. The Sun's luminosity (energy output), temperature, pressure, and composition all vary with depth in its interior. At the Sun's center, the pressure is 233 billion times that of the Earth's atmosphere at sea level.

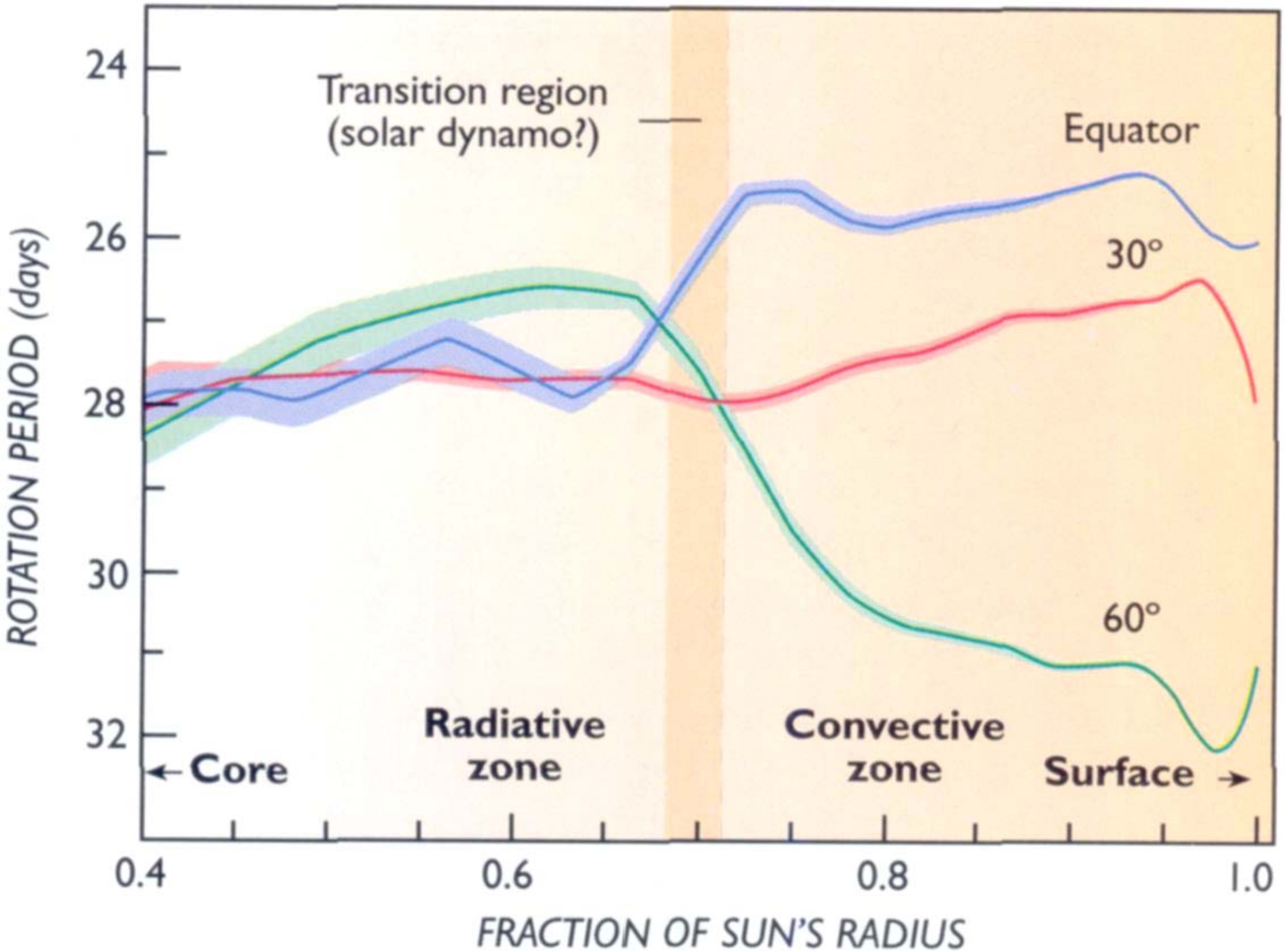

Figure 16. Internal rotation rates of the Sun at latitudes of 0°, 30°, and 60° have been inferred using data from the Michelson Doppler Imager (MDI) aboard the SOHO spacecraft. Just below the convection zone, the rotational speed changes markedly. Shearing motions along this interface may be the source of the Sun's magnetism.

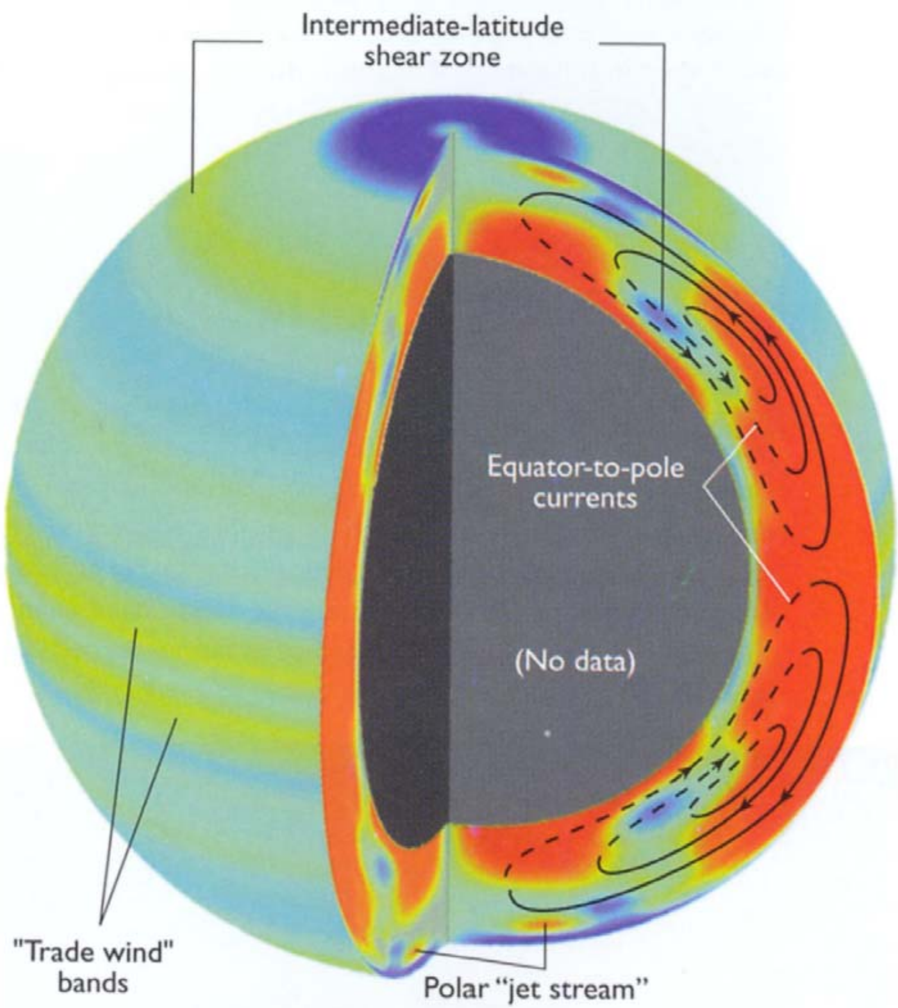

Figure 17. A surprising variety of large-scale flows occur in the Sun's interior. Red corresponds to faster-than-average flows, yellow to slower than average, and blue to slower yet. For example, on the left side, deeply rooted zones (yellow bands), analogous to the Earth's trade winds, travel slightly faster than their surroundings (blue regions). Sunspots may tend to form at the edges of these zones. Polar "jet streams" (dark blue ovals) move approximately 10 percent faster than their surroundings (light blue). There is slow movement poleward from the equator shown by the streamlines in the right-hand cutaway (the return flow below it is inferred).

Granular convection and sunspots as seen at 304 Angstroms

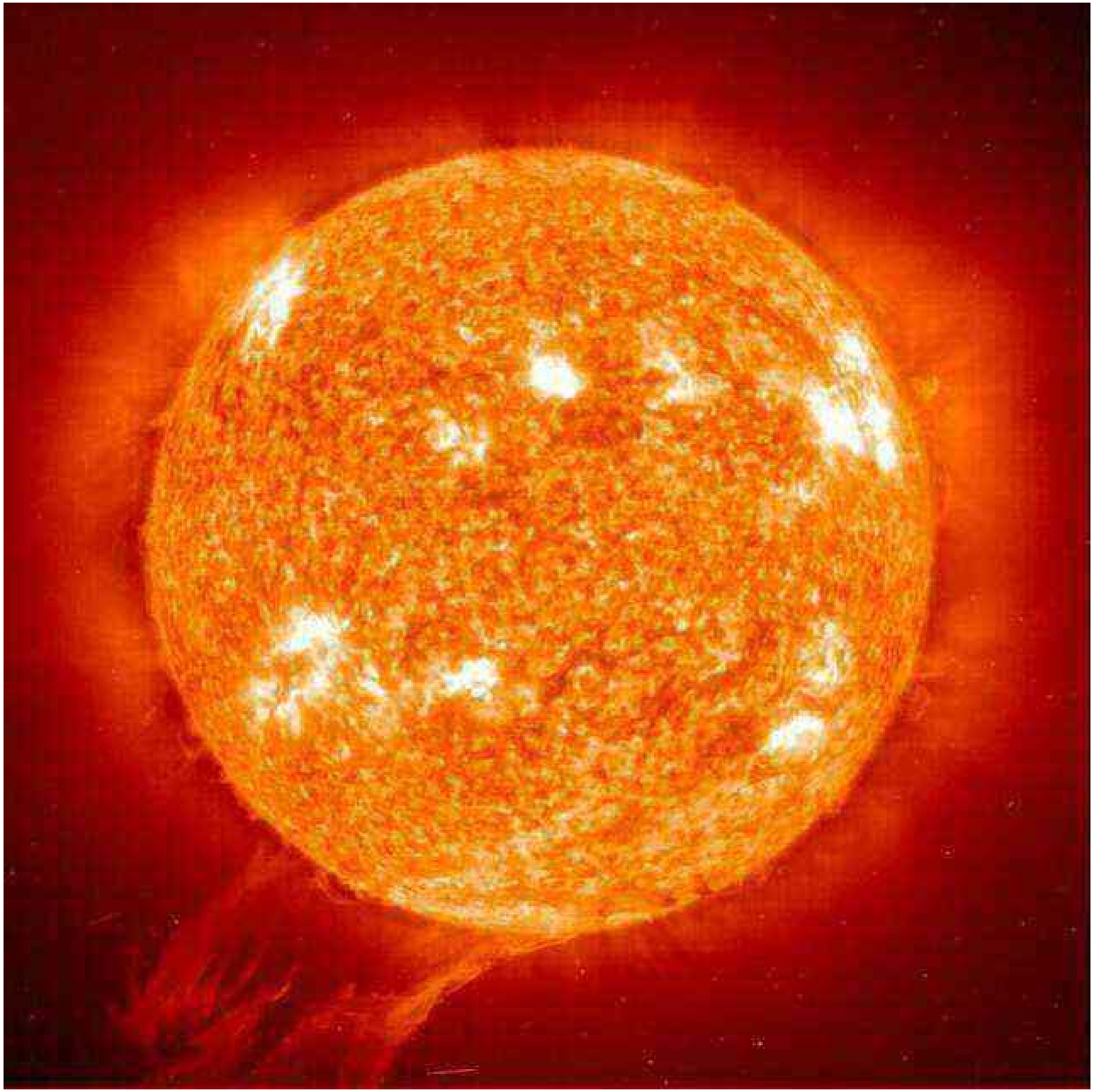

Sun, as seen in the far ultraviolet (195 Angstroms)

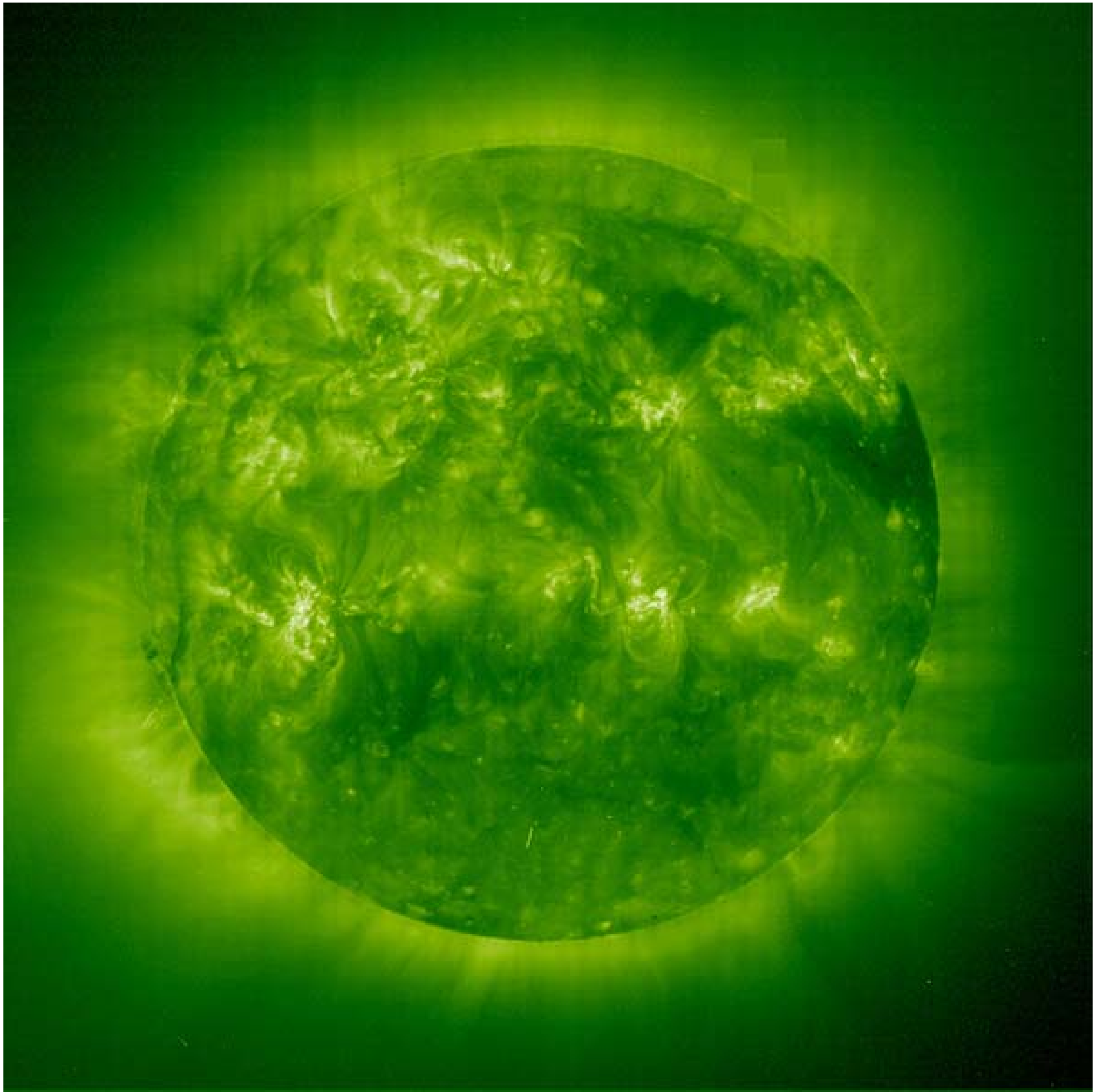

Prominences:

Magnetohydrodynamically controlled

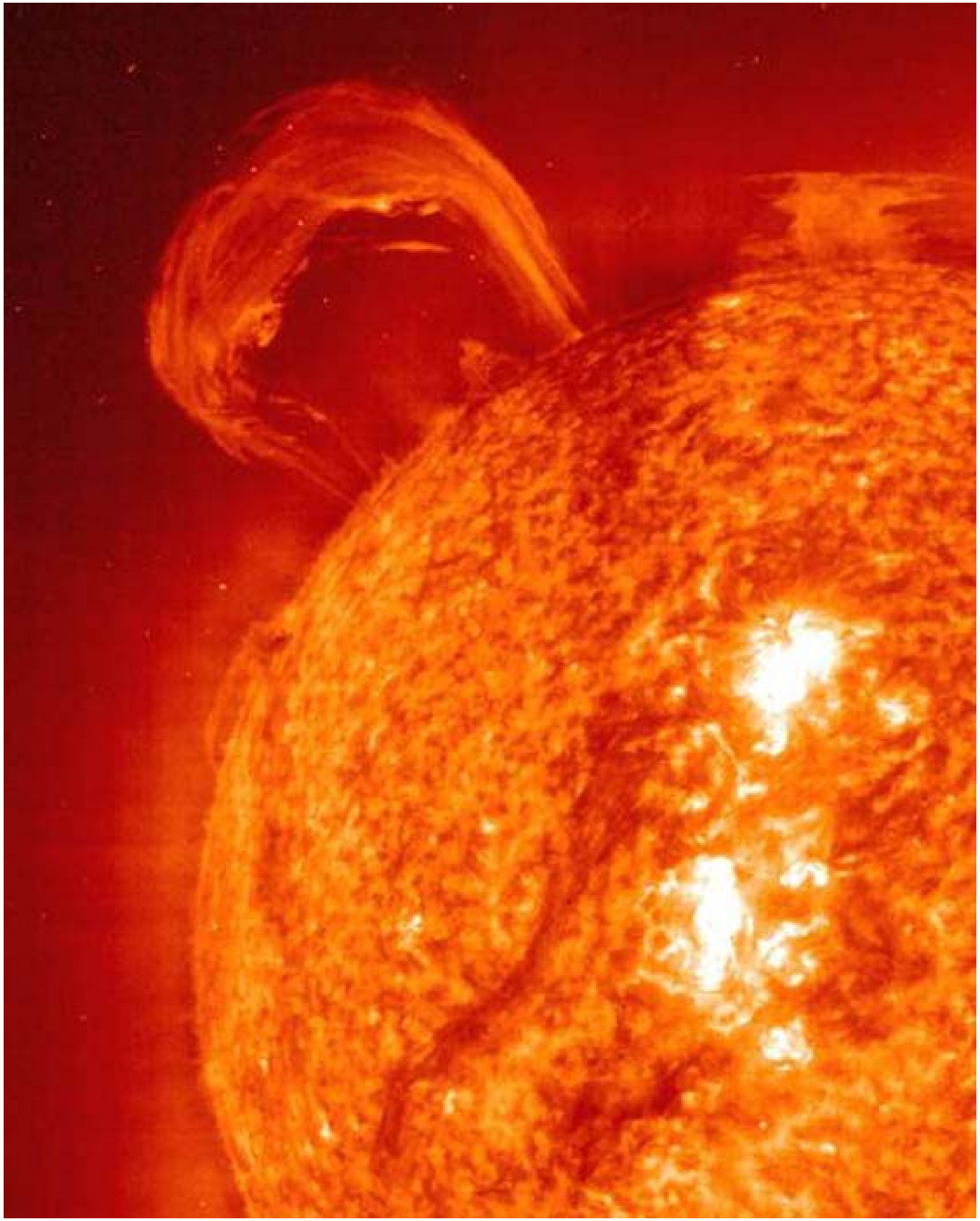

Solar disturbances and coronal looping, as seen by a soft X-ray satellite-borne telescope

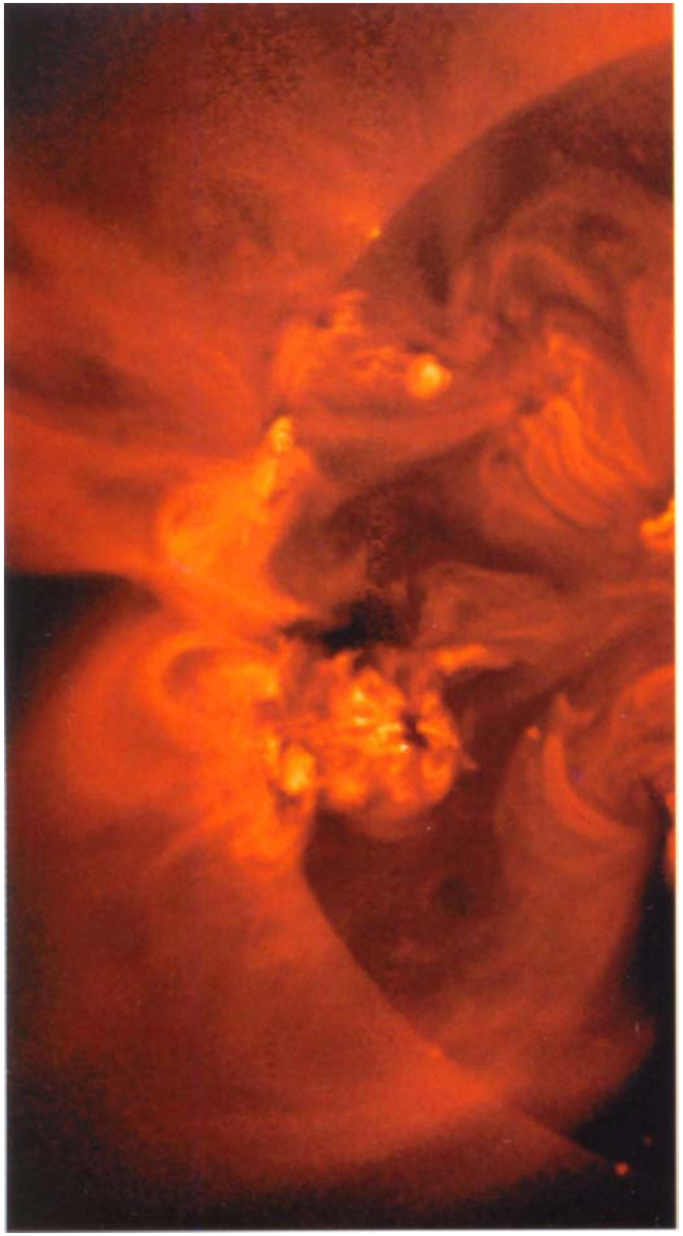

Solar corona as seen during a solar eclipse

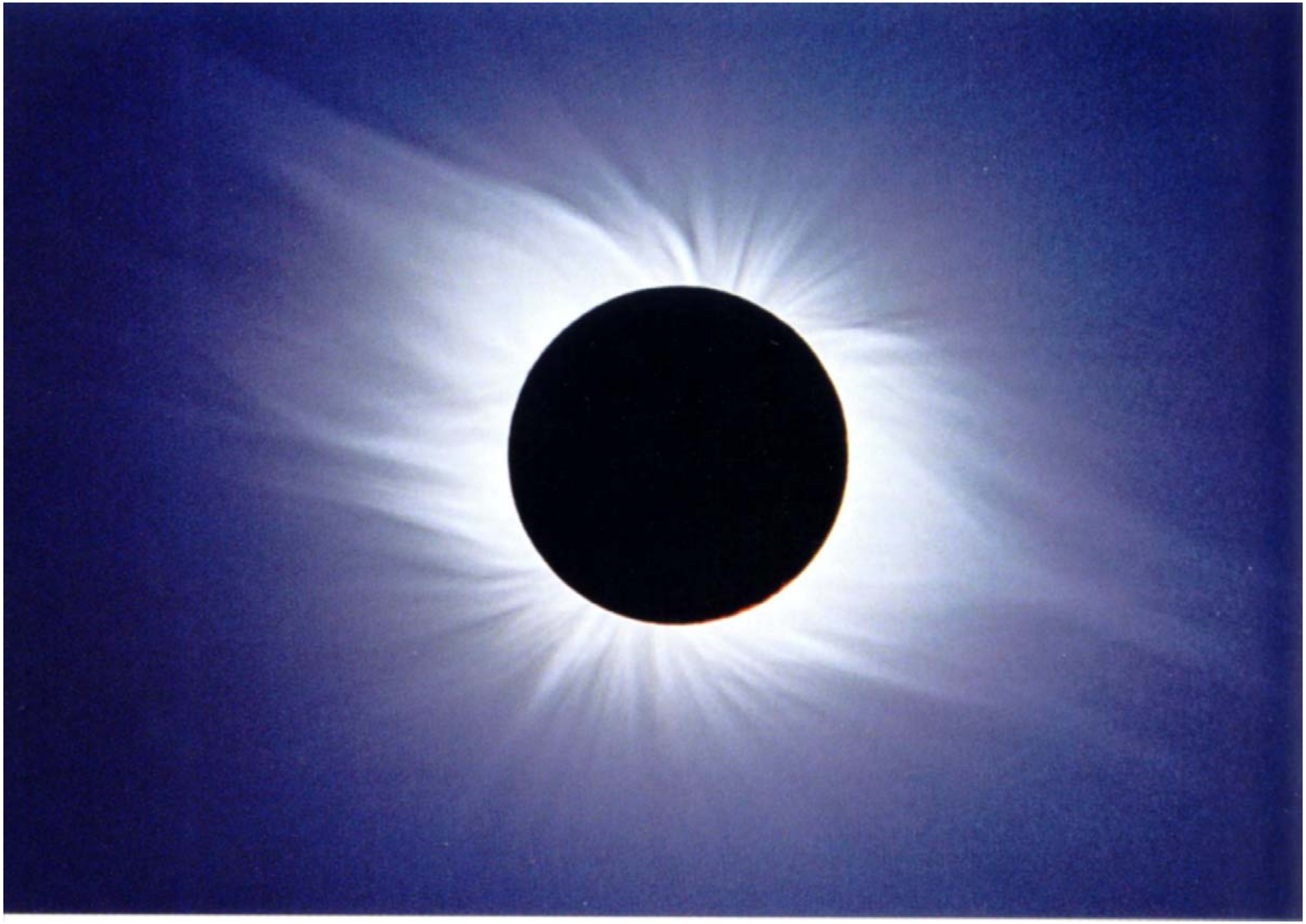

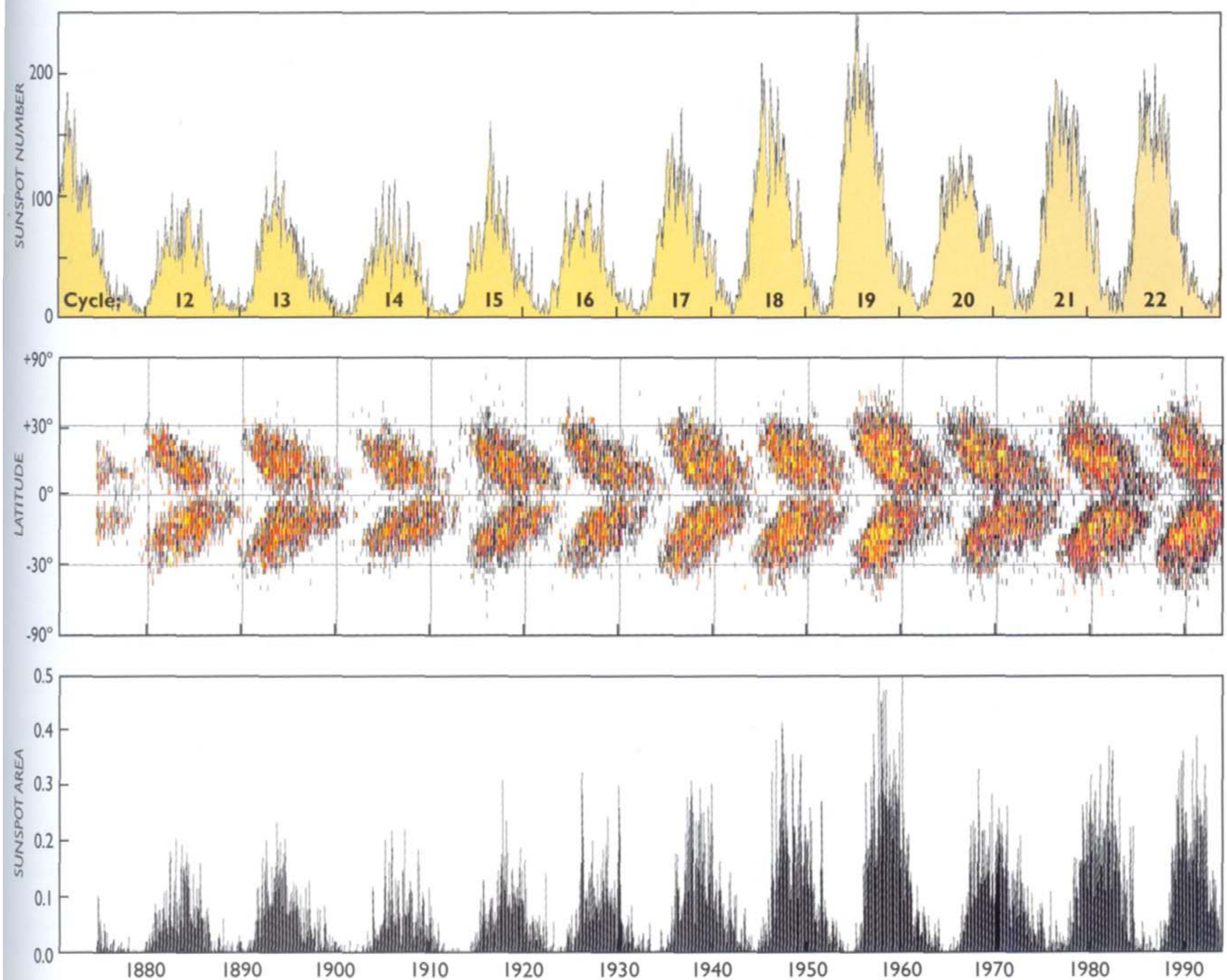

SUNSPOT NUMBER
200
100
0
Cycle:
12
13
14
15
16
17
18
19
20
21
22
LATITUDE
+90°
+30°
0°
-30°
-90°
SUNSPOT AREA
0.5
0.4
0.3
0.2
0.1
0.0
1880
1890
1900
1910
1920
1930
1940
1950
1960
1970
1980
1990

No generally accepted theory for short term variations in solar luminosity

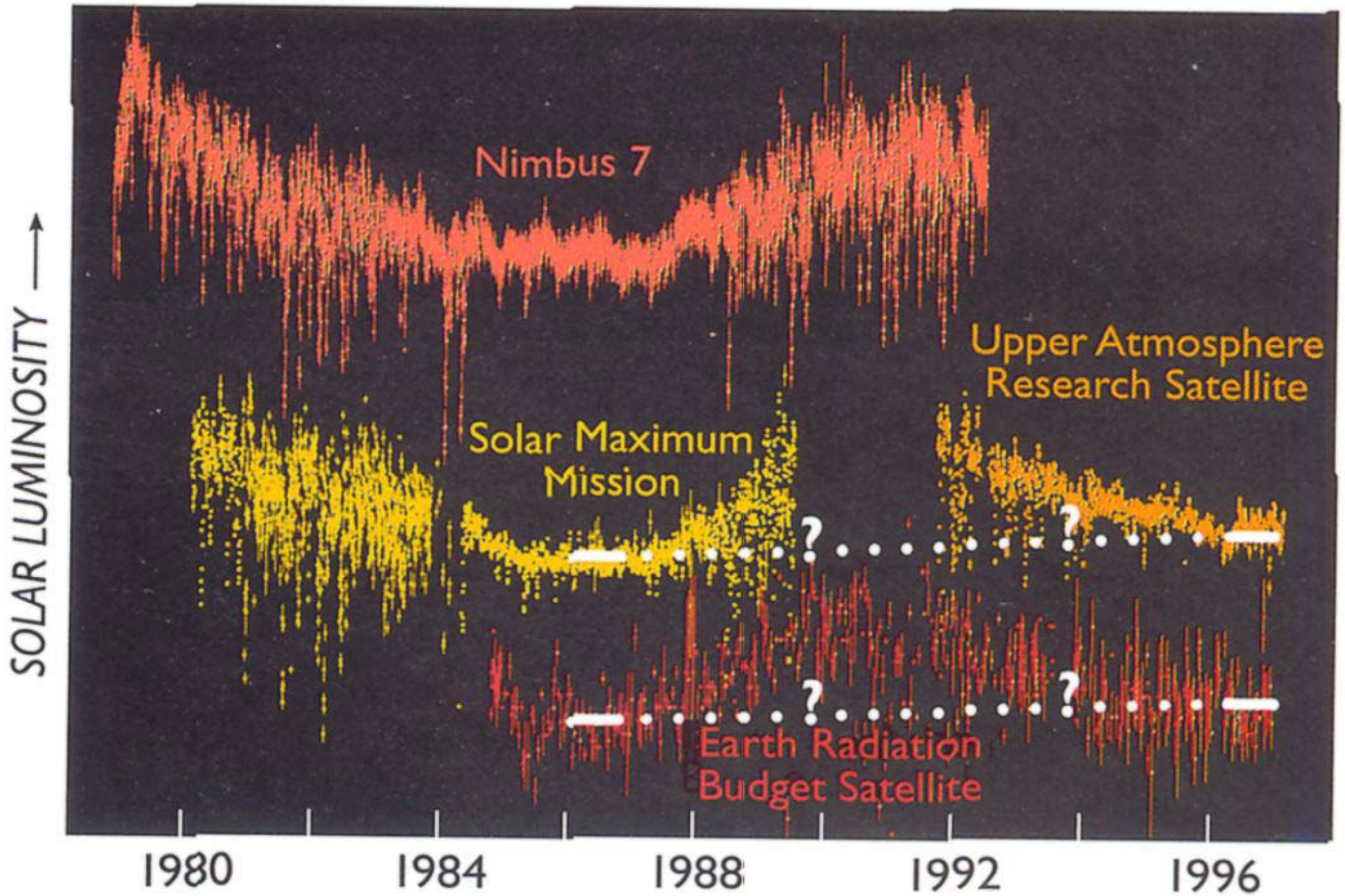

Figure 22. Complementary observations from several satellites show that the Sun's output fluctuates during each 11-year cycle (dips in curves), with a maximum coinciding with the peak in sunspot and magnetic activity. Some researchers believe the satellite data also suggest that the Sun was slightly brighter in 1996 than during the previous solar minimum (dashed lines). However, this interpretation is considered controversial, and a longer baseline of observations is needed.

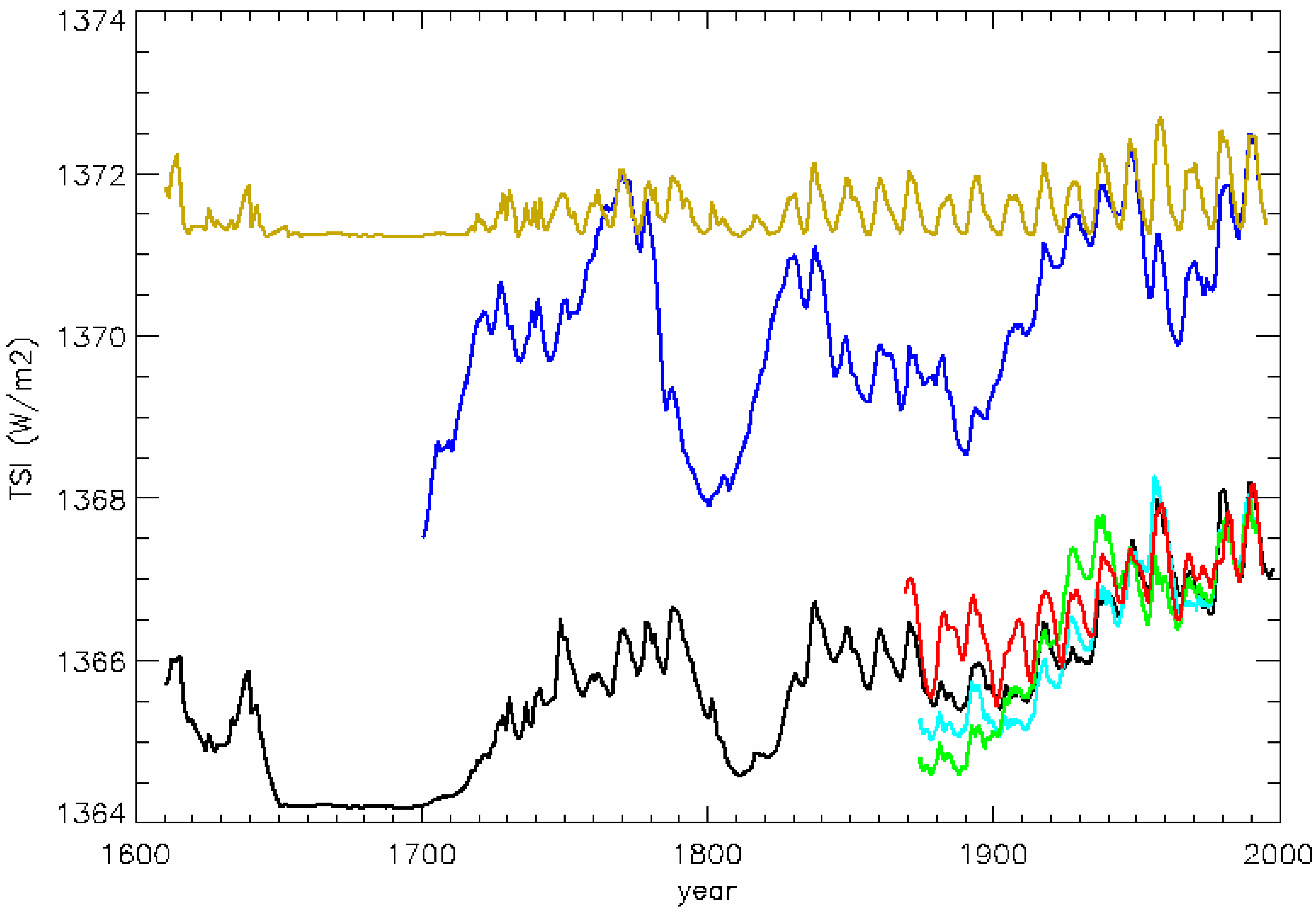

Fig. 6.6: Reconstructions of total solar irradiance by: blue - Hoyt and Schatten (1993), black - Lean, Beer and Bradley (1995), cyan - Solanki and Fligge (1998) version A, green - ditto version B, red - Lockwood and Stamper (1999), yellow - group sunspot numbers (Hoyt and Schatten, 1998) scaled to Nimbus-7 observations for 1979-1993.

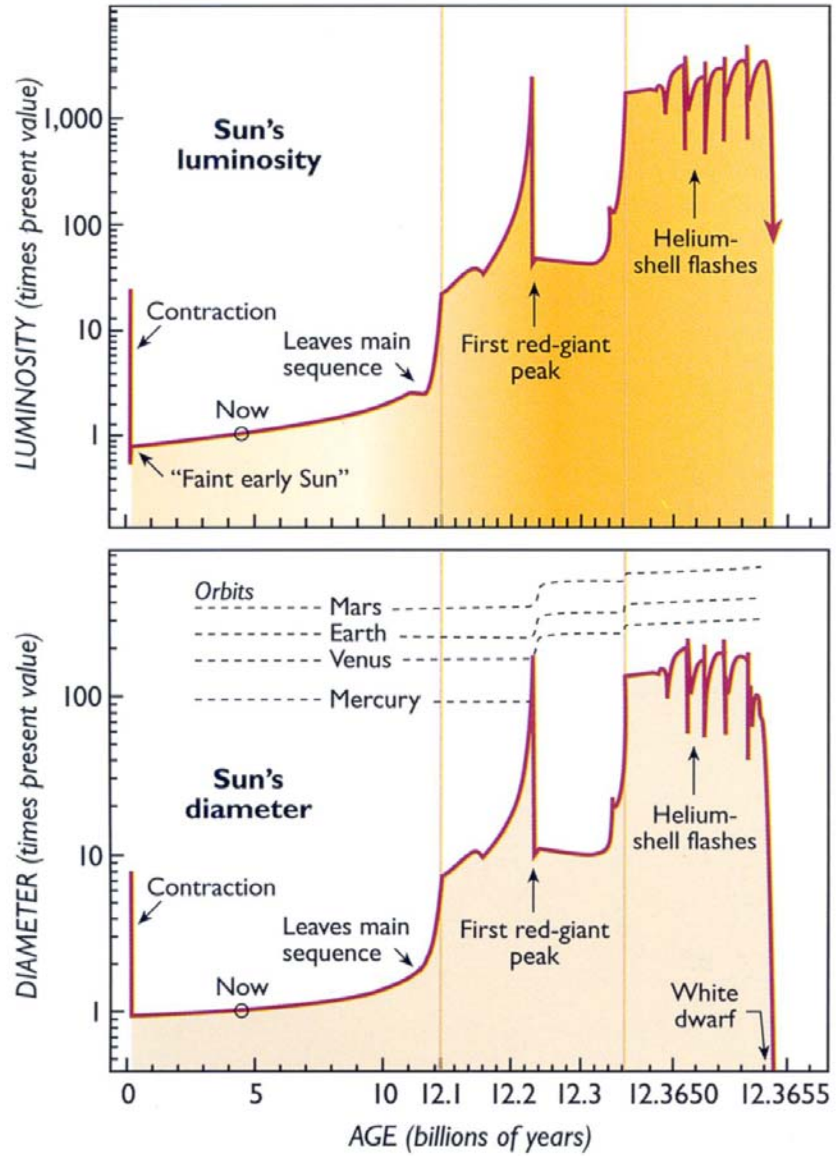

Figure 24. Billions of years from now the Sun will grow enormously in size and luminosity. Note the different time scales, expanded near the end of the Sun's life to show relatively rapid changes. The orbits of the planets enlarge due to mass loss from the Sun. By the time our star becomes a white dwarf, it will have only 0.51 to 0.58 of its present mass.

Supernovae: Absorption of neutrinos produces shock wave that blows off envelope of gas. Shock wave stops at finite radius…envelope should then collapse but does not…..

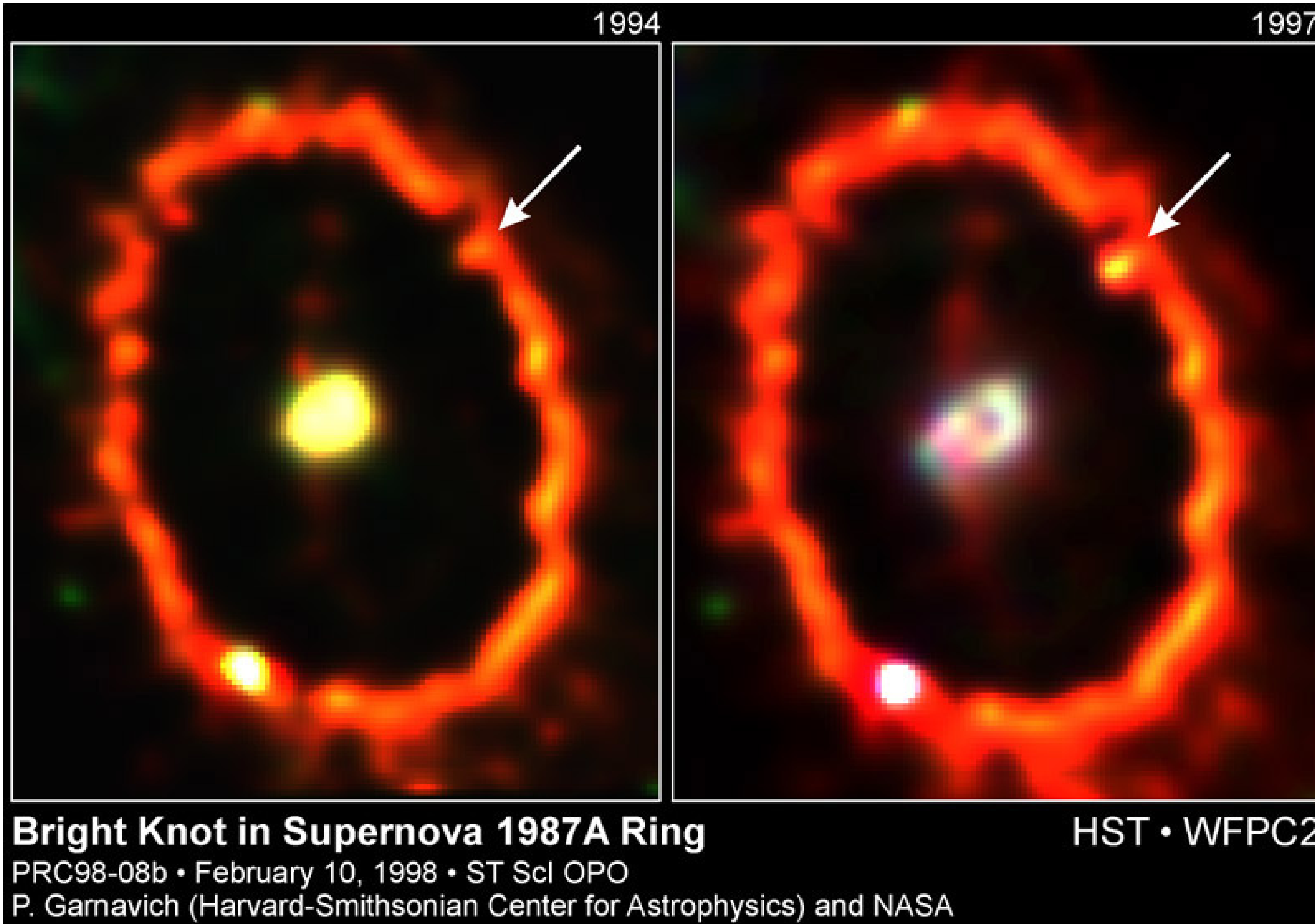

2. Mantle Convection

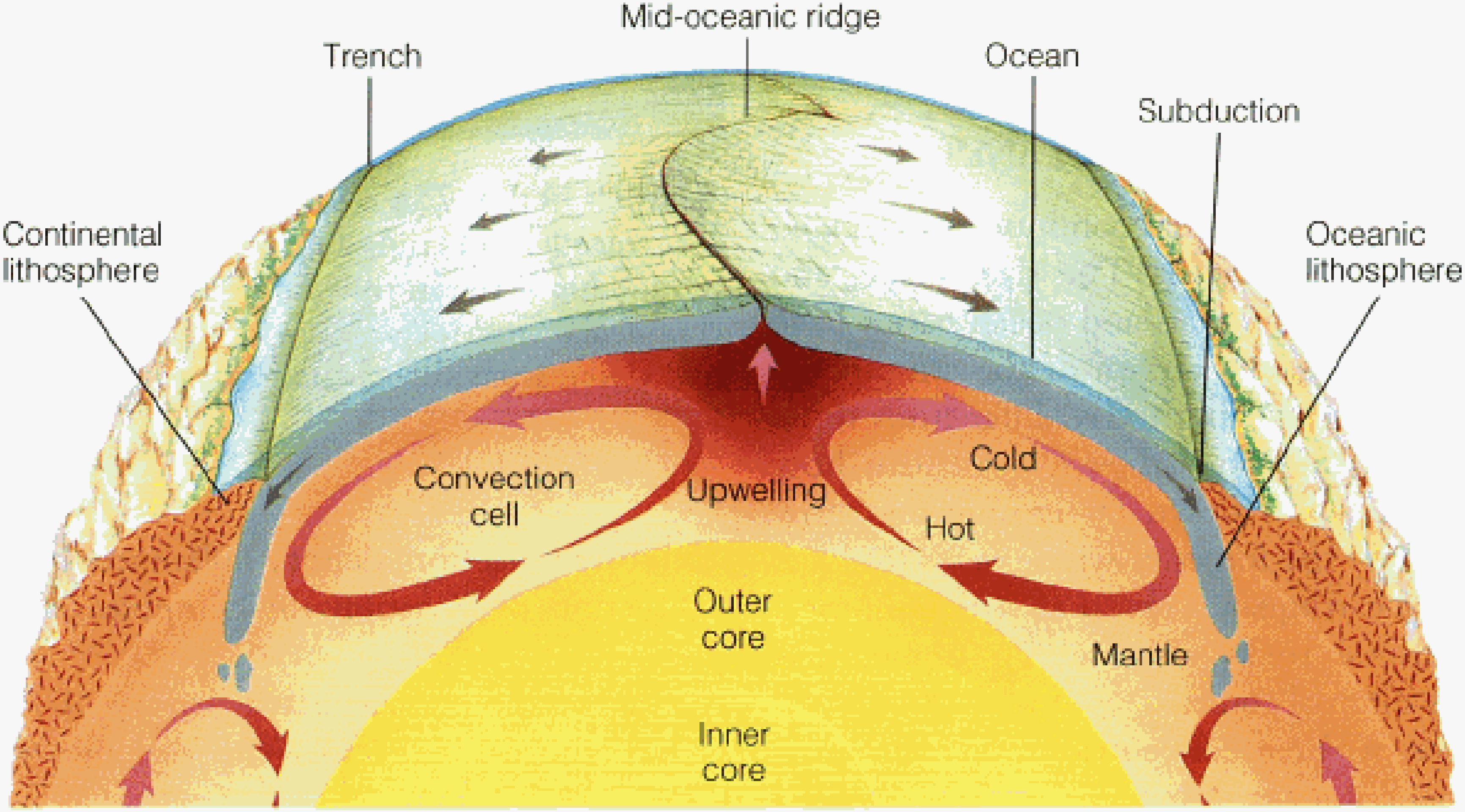
Mid-oceanic ridge
Trench
Ocean
Subduction
Continental lithosphere
Oceanic lithosphere
Convection cell
Upwelling
Cold
Hot
Outer core
Mantle
Inner core

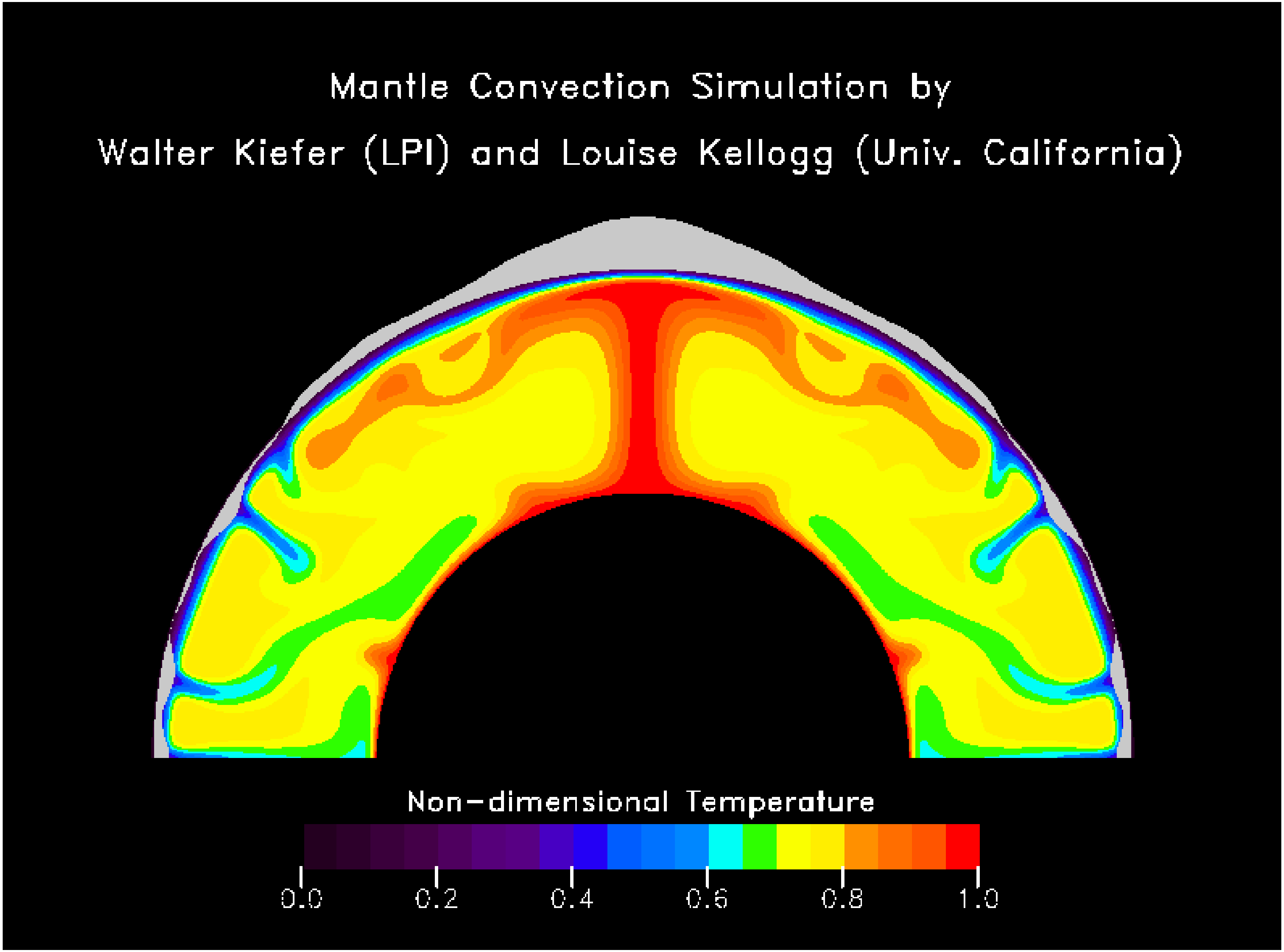
Mantle Convection Simulation by
Walter Kiefer (LPI) and Louise Kellogg (Univ. California)
Non-dimensional Temperature
0.0
0.2
0.4
0.6
0.8
1.0

3. Climate Dynamics

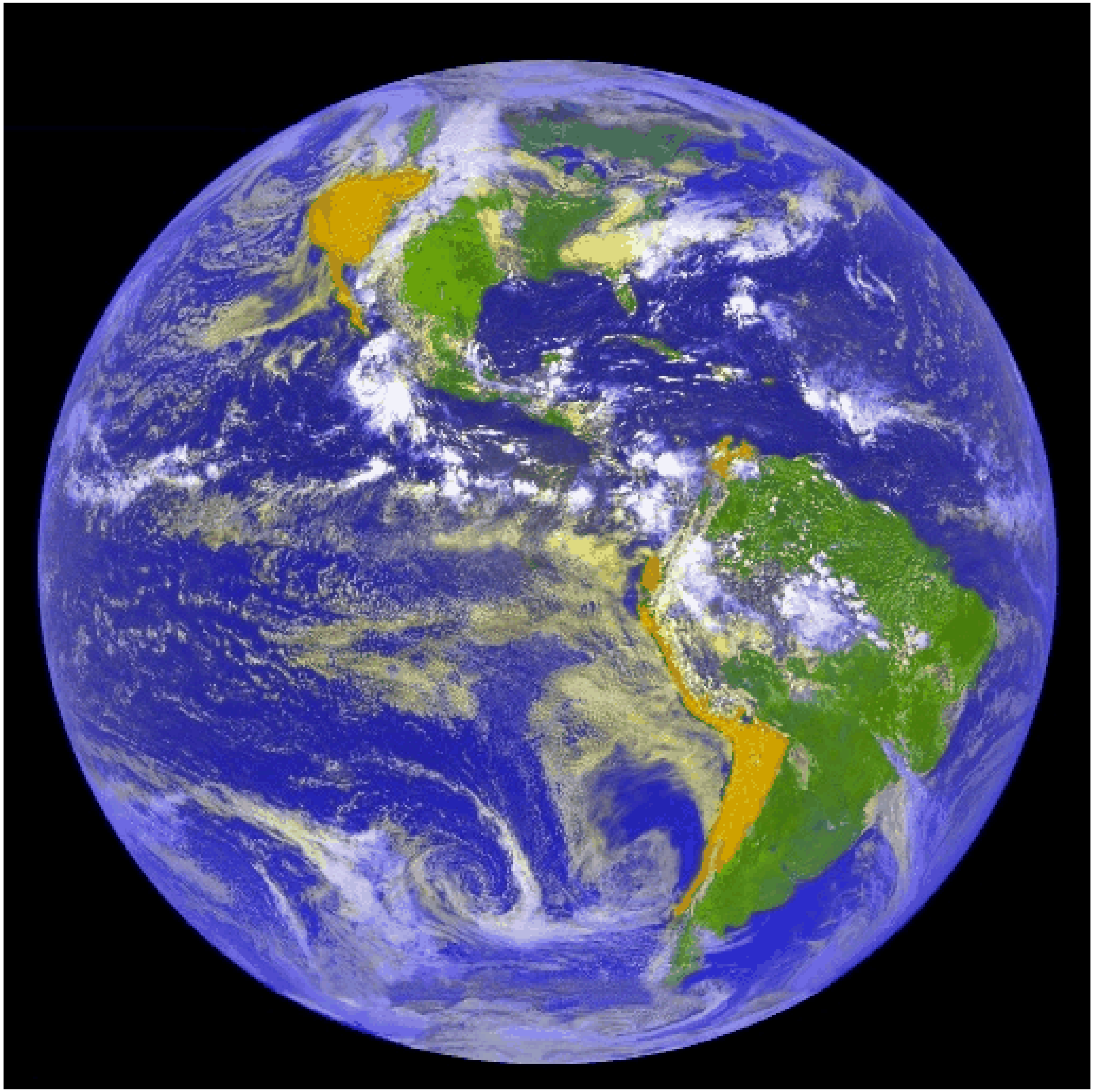

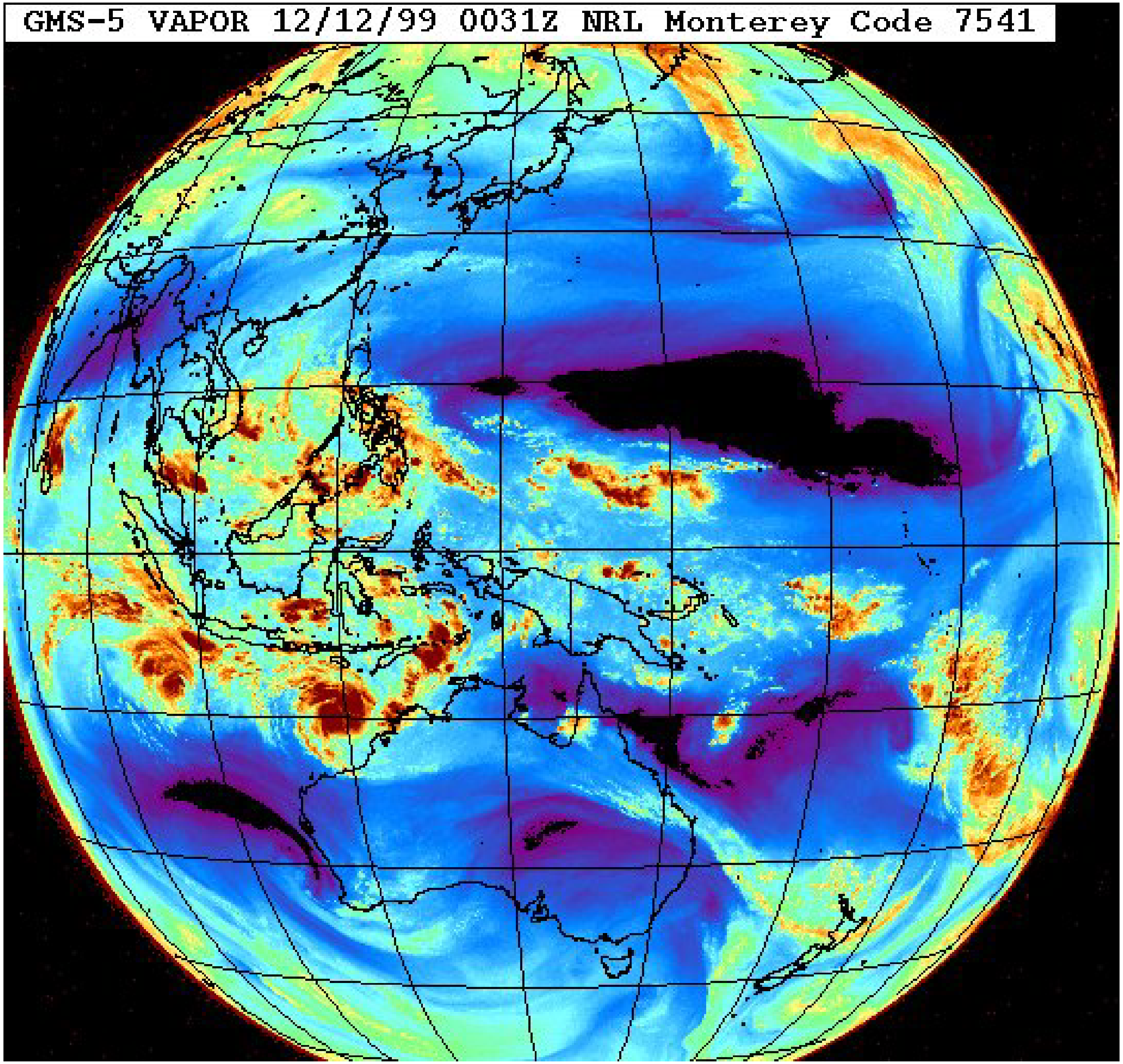
GMS-5 VAPOR 12/12/99 0031Z NRL Monterey Code 7541

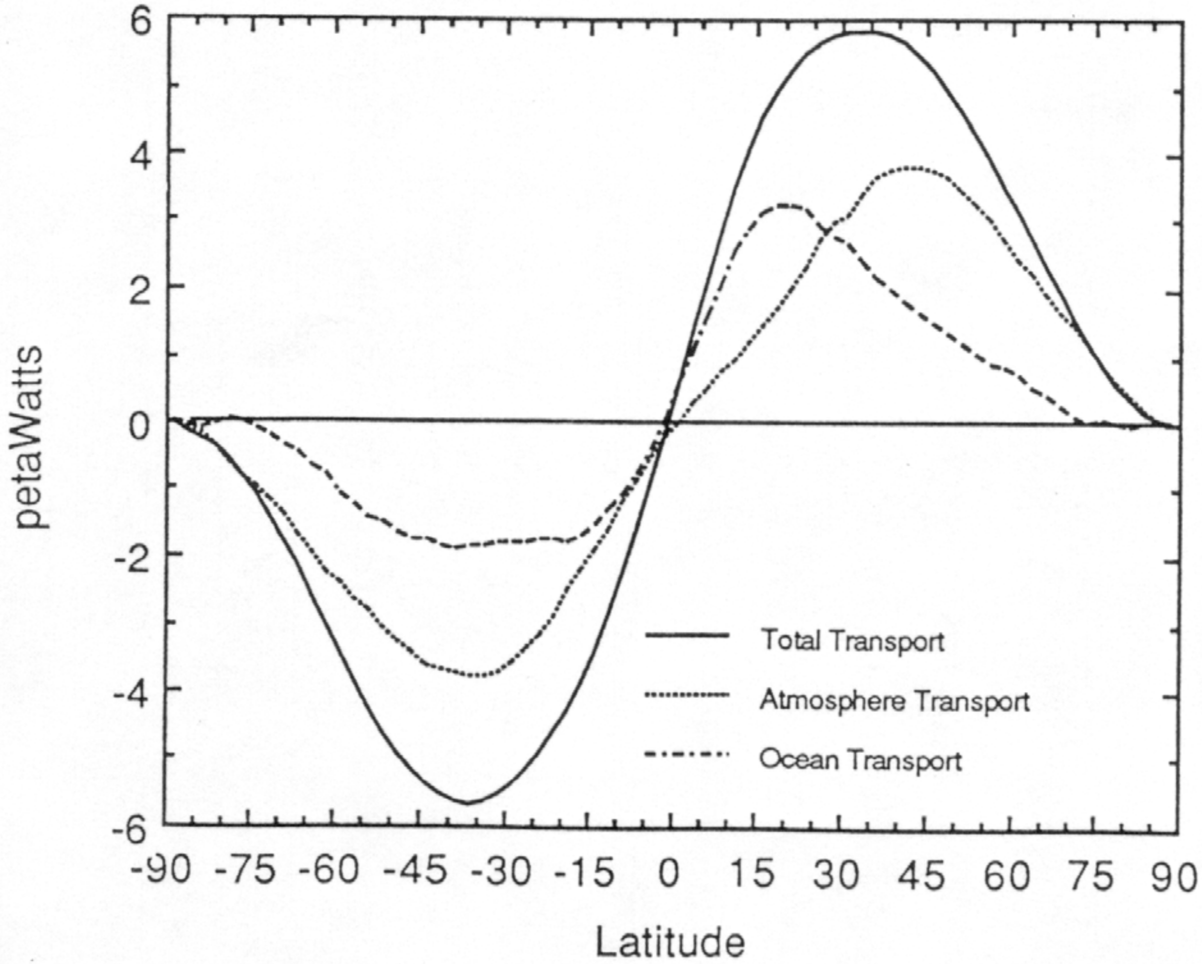

Heat Transport by Oceans and Atmosphere

Ocean Thermohaline Circulation

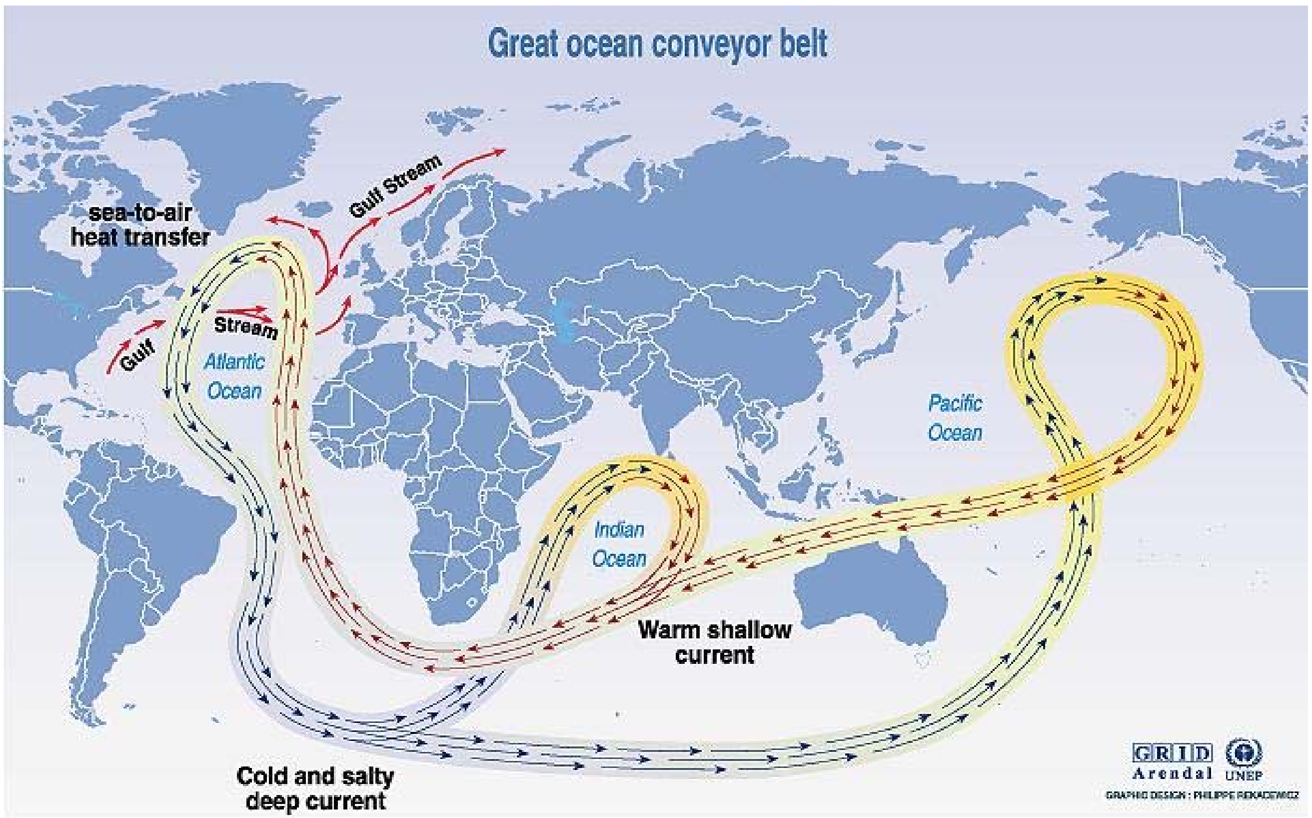

Source: Broecker, 1991, in Climate change 1995, Impacts, adaptations and mitigation of climate change: scientific-technical analyses, contribution of working group 2 to the second assessment report of the intergovernmental panel on climate change, UNEP and WMO, Cambridge press university, 1996.

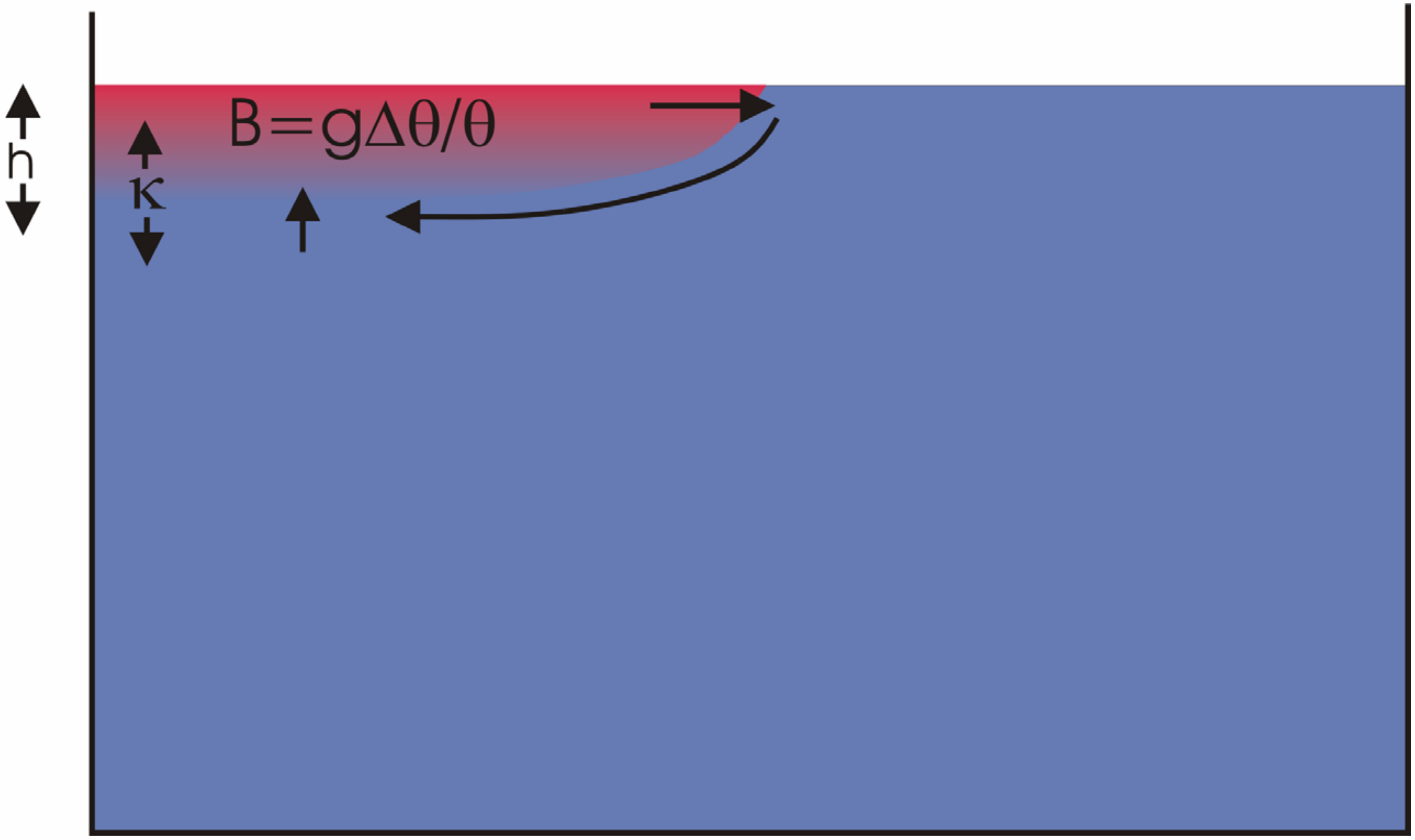

A hot plate is brought in contact with the left half of the surface of a swimming pool of cold water. Heat diffuses downward and the warm water begins to rise. The strength of the circulation is controlled in part by the rate of heat diffusion. In the real world, this rate is very, very small.

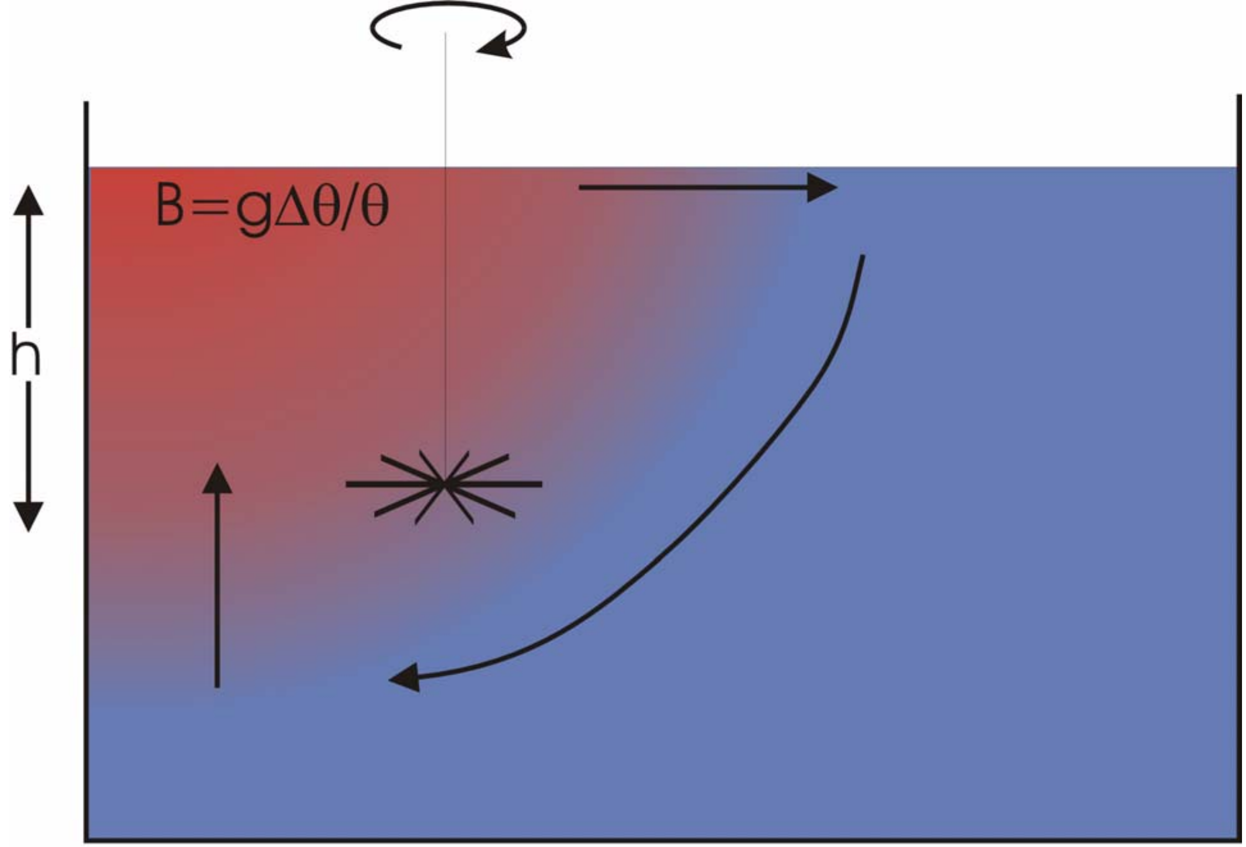

$$\text{Heat Flux} \sim P^{2/3} B^{2/3}$$

$$h \sim P^{1/3} B^{-2/3}$$

Adding a stirring rod to this picture greatly enhances the circulation by mixing the warm water to greater depth and bringing more cold water in contact with the plate. The strength of the lateral heat flux is proportional to the 2/3 power of the power put into the stirring, and the 2/3 power of the temperature of the plate.

ISS007E14883

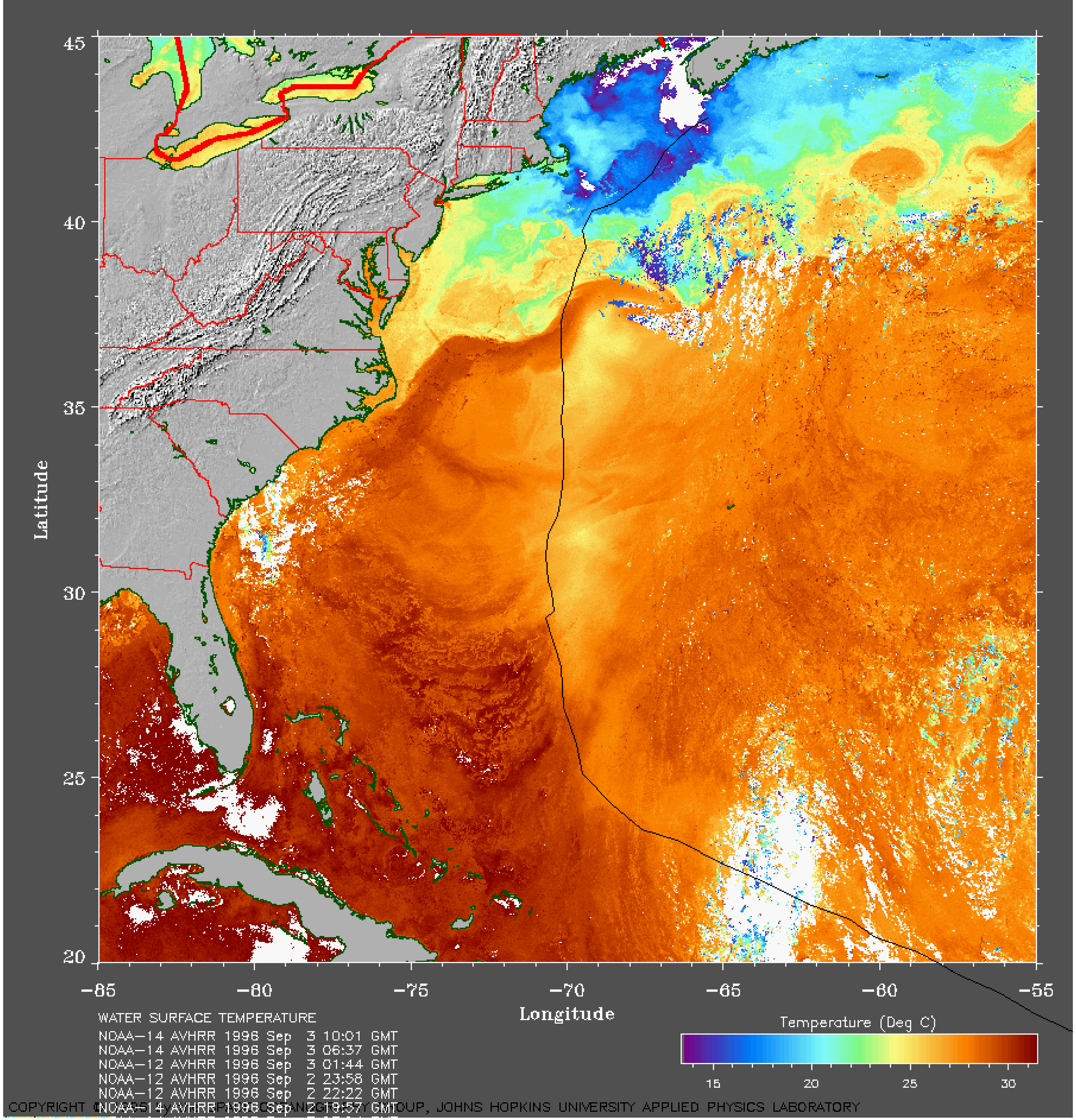
45
40
35
30
25
20
Latitude
-85
-80
-75
-70
-65
-60
-55
Longitude
WATER SURFACE TEMPERATURE
NOAA-14 AVHRR 1996 Sep 3 10:01 GMT
NOAA-14 AVHRR 1996 Sep 3 06:37 GMT
NOAA-12 AVHRR 1996 Sep 3 01:44 GMT
NOAA-12 AVHRR 1996 Sep 2 23:58 GMT
NOAA-12 AVHRR 1996 Sep 2 22:22 GMT
NOAA-14 AVHRR 1996 Sep 2 19:57 GMT
Temperature (Deg C)
15
20
25
30
JOHNS HOPKINS UNIVERSITY APPLIED PHYSICS LABORATORY

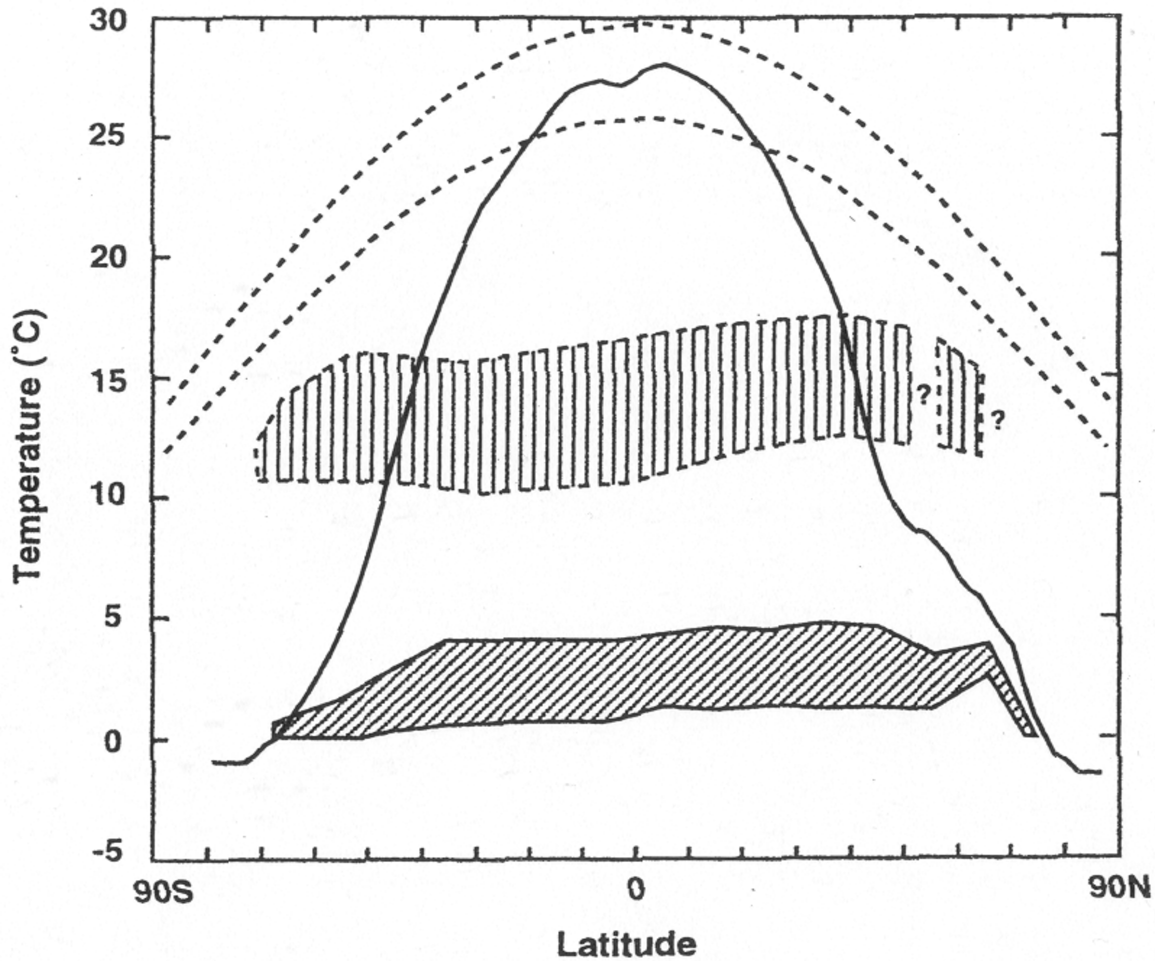

Figure 4.1. Modern (solid line) and estimated early Eocene (dashed lines) zonal sea surface temperatures. Modern (diagonal hatch) and estimated early Eocene (vertical hatch) water temperatures at bottom depths between 1000 m and 5000 m. Modern data are from the *World Ocean Atlas data set* (Levitus and Boyer, 1994). The cooler Eocene SST profile is based on Zachos *et al.* (1994); the warmer SST profile is based on Crowley and Zachos (Chapter 3, this volume).